ISSN 0869-5911, Petrology, 2008, Vol. 16, No. 3, pp. 299–311. © Pleiades Publishing, Ltd., 2008.
Original Russian Text © E.V. Badanina, L.F. Syritso, V.S. Abushkevich, R. Thomas, R.B. Trumbull, 2008, published in Petrologiya, 2008, Vol. 16, No. 3, pp. 317–330.

Geochemistry of Ultra-Potassic Rhyodacite Magmas from the Area of the Orlovka Massif of Li–F Granites in Eastern Transbaikalia: Evidence from Study of Melt Inclusions in Quartz

E. V. Badanina[a], L. F. Syritso[b], V. S. Abushkevich[c], R. Thomas[d], and R. B. Trumbull[d]

[a] *Geological Department, St.-Petersburg State University, Universitetskaya nab. 7/9, St. Petersburg, 199034, Russia*
e-mail: elena_badanina@mail.ru

[b] *Scientific Research Institute of the Earth Crust, Universitetskaya nab. 7/9, St. Petersburg, 199034, Russia*

[c] *Institute of Precambrian Geology and Geochronology, Russian Academy of Sciences, nab. Makarova 2, St. Petersburg, 199034 Russia*
e-mail: vik2211@rol.ru

[d] *GeoForschungsZentrum Potsdam, Telegrafenberg, D-14473, Potsdam Germany*

Received October 13, 2006; in final form, March 15, 2007

Abstract—Dikes, stocks and/or sheet flows of felsic volcanic and subvolcanic rocks are typically observed in the vicinity of rare-metal Li–F granite massifs. Their ubiquitous spatial association to rare-metal granites and, often, geochemical affinity to them suggest their certain petrological relation. Compositionally unique ultrapotassic trachydacites enriched in many rare elements were found among these rocks within the Khangilay complex of ore deposits in Eastern Transbaikalia. Melt inclusions in rock-forming quartz were studied to reconstruct the composition and evolution of parent melt. The obtained data demonstrated the existence of a super-potassic peraluminous melt (K_2O = 6.12 wt %, Na_2O = 1.08 wt %) having elevated contents of rare lithophile elements (730 ppm Rb_2O and 900 ppm BaO). The ion-microprobe content of Li is 354.23 ppm at a relatively low F content (up to 0.5 wt %). The residual melt is characterized by the most unusual composition: extremely low contents of mafic components and basicity (< 0.5 wt % femic oxides), a high Al index (A/CNK = 1.53) at comparatively low SiO_2 (60 wt %), and high total sodic alkalinity (more than 10 wt % $K_2O + Na_2O$; 6.11 wt % Na_2O). Such a composition corresponds to ongonite magma. However, the melt contains no F but has a high Cl content (0.34 wt %), which corresponds to the limit Cl saturation of haplogranite melt. SHRIMP-II U–Pb zircon dating showed significant difference between rare metal granites and trachyrhyodacites of the Khangilay complex of ore deposits: 139.9 ± 1.9 Ma and 253.4 ± 2.4 Ma, respectively. The geochemical similarity of these rocks, primarily in terms of abundance of refractory elements, REE distribution patterns, and initial Sr ratio, indicates their derivation from similar protolith.

DOI: 10.1134/S0869591108030053

INTRODUCTION

Recent years were marked by keen interest in subvolcanic and volcanic felsic rocks, that are often volatile-rich and accompanied by productive ore mineralization (Be, Sn, U, Mo, and W) (Kovalenko and Kovalenko, 1976; Burt et al., 1982; Christiansen et al., 1986; Kortemeir and Burt, 1988; Chabiron et al., 2001; Antipin et al., 2002). These rocks compose dikes, stocks, and thin flows and show extremely wide compositional variations and different geochemical and metallogenic specialization. This extremely complicates the classification of these rocks with known rock types: ongonites, elvanes, ongorhyolites, and topaz rhyolites. New varieties of subvolcanic rocks recently found at numerous localities worldwide have no analogues in the available classification schemes and are termed by local names: selengite (Kozlov et al., 1983), djumalite (Dergachev, 1989), kalgutite (Titov et al., 2001), macusanite (Pichavant et al., 1987), xianghualingite (Zhu and Zhang, 2003), and others. This highlights the need for a more universal classification and nomenclature of the rocks as compared with the earlier scheme based on the degree of crystallization, Na/K ratio, and contents of F, B, and P (Dergachev, 1992). Taking into account the different contribution of magmatic and metasomatic process to the formation of these rocks, two avenues can be proposed to develop this classification. The study of melt inclusions makes it possible to exclude a metasomatic overprint (Naumov et al., 1984; Webster et al., 1996), while the isotopic–geochemical approach yields age relations between subvolcanic and volcanic rocks, including granitoid magmatism, as well as reliable data on the melt source.

In this paper, this approach was applied for the first time to specific subvolcanic rocks, ultrapotassic trachyrhyodacites, which occur in the Khangilay complex of rare-metal ore deposits in eastern Transbaikalia. The chemistries of these rocks are discussed in (Syritso et

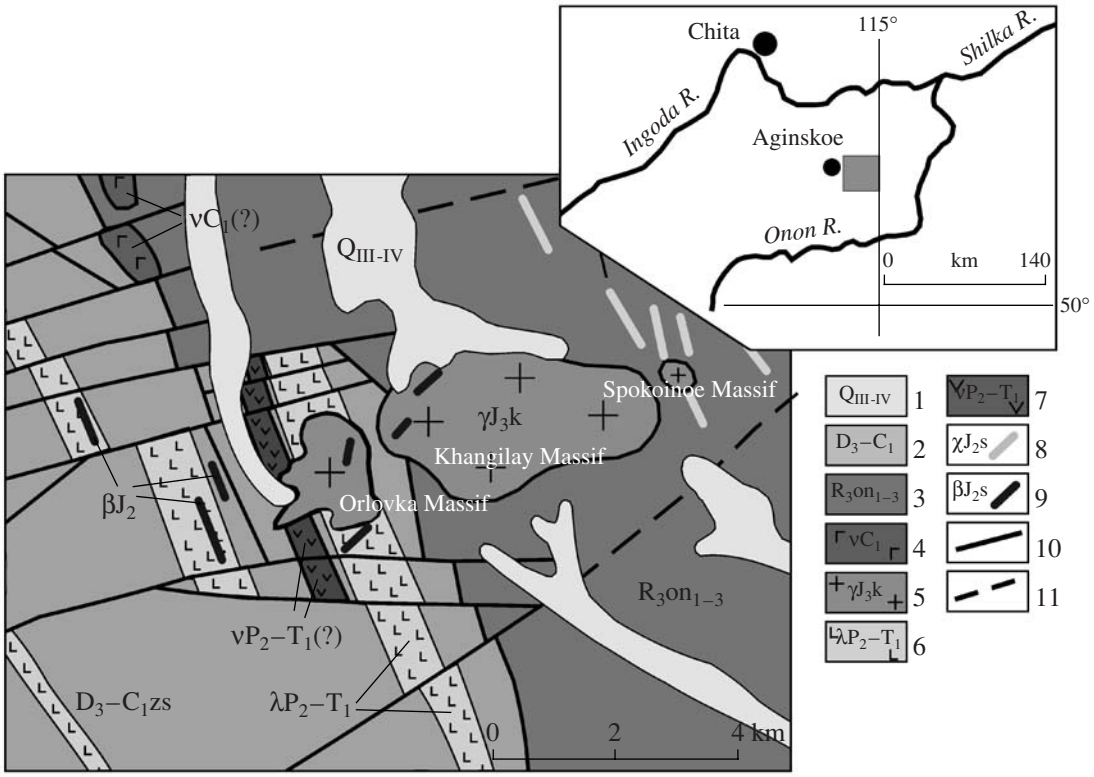

Fig. 1. Schematic geological map of the Khangilay ore cluster (modified after report Krivitskii et al., 2001).
(1) Quaternary deposits; (2) Upper Devonian–Lower Carboniferous gravelstones, sandstones, and siltstones; (3) Upper Riphean sandstones and silty pelites; (4) Early Carboniferous (?) subalkaline gabbro (Inkizhin stocks); (5) Late Jurassic granites of the Kukulíbei Complex (Khangilay intrusion); (6–9) rocks of the dike complex: (6) Late Permian–Early Triassic trachydacites and trachyrhyolites; (7) Late Permian–Early Triassic (?) diabases; (8) Middle Jurassic (kersantite and spessartite); (9) Middle Jurassic dolerites, (10, 11) faults. Lamprophyres and dolerite dikes are shown beyond the scale.

al., 2005). As was mentioned previously, their geochemical specialization reflects the contrasting enrichment, on the one hand, in rare lithophile elements (Rb, Li, Cs, and F), as is typical of rare-metal granites of the Orlovka Massif, and, on the other hand, in refractory elements (Zr, Nb, Ta, and REE), which are typical of the subalkaline basaltic dikes of the ore cluster. The geochemical affinity of these rocks with rare metal granites and their spatial association not only in the Khangilay complex but also in other groups of deposits of Transbaikalia (Sherlovogorskoe, Shumilovka, and Bukuka–Belukha), and even in other rare-metal Phanerozoic provinces (Voznesenka in Primorye) suggests their unambiguous petrological relation. The knowledge of this relation can provide insight into the conditions under which felsic rare-metal magmas are formed.

The Orlovka trachyrhyodacites have an unusual chemical composition, in particular, an extremely high K content. Therefore, in order to decipher their genesis, we first estimate the composition of primary melt and exclude the metasomatic overprint. To reconstruct the composition and possible crystallization evolution of the primary melt, we studied melt inclusions in the rock-forming quartz. The results of this study are reported below.

PETROGRAPHY AND MINERAL COMPOSITION

Since the geology of the Khangilay complex (Beskin et al., 1994; Syritso et al., 2001) and the mineral and chemical composition of trachyrhyodacites and trachyrhyolites were reported elsewhere (Syritso et al., 2005), below we consider only some structural and compositional features, which were obtained later and are of principal significance for discussing the formulated problem. A geological map of the area with outlines of trachyrhyodacite bodies is shown in Fig. 1. It should be noted that these rocks occur only near the amazonite granites of the Orlovka Massif and were not found near the parent Khangilay Massif and the Spokoinoe satellite. The trachyrhyodacites have no direct contacts with the granites of the Orlovka Massif, but the light trachyrhyodacites are sometimes cut by porphyroblastic granites with snowball quartz. More detailed geological observations showed that the trachydacite and trachyrhyolite bodies are not dikes in a general sense; they have no distinct contacts and, in

terms of relations with the host sandy–shaly rocks, can be considered as a dike-shaped inclined body 70–90 m in apparent thickness and up to 800 m long. In its central part, these rocks resemble subvolcanic rocks in having a porphyritic texture with phenocrysts of K-feldspar (KFsp) and quartz, elements of a fluidal structure, and sandy–shaly clasts. The rocks are vitrophyric with domains of weakly recrystallized glass. According to their appearance, they are subdivisible into two varieties showing gradual transitions: dark almost black fine- to medium-grained rocks with phenocrysts of light KFsp and light fine-grained rocks with ovoid phenocrysts of quartz and KFsp. As will be shown below, the dark rocks chemically correspond to trachydacite, while the light rocks are classed with trachyrhyolite. The dark trachydacite contains rounded perlites 0.08–0.1 mm in size, which are in places recrystallized into a microfelsitic quartz–feldspar aggregate. The rocks also contain characteristic KFsp spherulites 0.05–0.1 mm in size. In appearance (grain size, euhedrality), the KFsp is represented by two varieties: large (0.7 cm) euhedral phenocrysts with rudimentary microcline hatching and small anhedral grains in association with quartz and sodic plagioclase in the groundmass. The KFsp of the rhyolites shows more distinct microcline hatching. The crosscutting relations of fine granular groundmass to KFsp phenocrsysts indicate the early crystallization of the latter. This is also confirmed by the elevated Na content in the phenocryst KFsp as compared to that in the groundmass mineral. In spite of the same mineral composition [Kfsp 40–45%, quartz 35–45%, plagioclase (strongly sericitized) 10–15%, biotite, muscovite 2–3%, and glass up to 1%], the trachydacites and trachyrhyolites have significant differences. In particular, the trachydacites contain fine-flaked dark mica (Mg–Fe biotite) and amphibole, whereas the trachyrhyolites lack amphibole and contain light phengite–muscovite instead of dark mica. They also differ in the composition of their accessory minerals. The trachydacites contain apatite, zircon, monazite, and scarce titanite, whereas trachyrhyolites are dominated by topaz with subordinate amounts of apatite and zircon. The secondary minerals in both rocks are sericite, pelitic matter, and carbonate.

The results of microprobe analysis of major rock-forming minerals are listed in Tables 1 and 2. As is seen in Table 1, the mafic mica from the inclusions in rhyodacites corresponds to Mg–Fe biotite. Mica in the rock is significantly less magnesian and has a low F content (no higher than 0.33 wt %). The amphibole is represented by common hornblende (wt %): SiO_2 – 49.96, TiO_2 – 1.27, Al_2O_3 – 4.83, FeO_{tot} – 15.54, MnO – 0.39, MgO – 13.76, CaO – 11.53, Na_2O – 1.69, K_2O – 0.78. The K feldspar (Table 2) in the inclusions and rocks is similar in composition and contains a significant admixture of W (up to 0.11 wt % WO_3) and Ta (up to 0.08 wt % Ta_2O_5). Small unaltered plagioclase grains in the groundmass are practically pure albite. Unlike KFsp, plagioclase ubiquitously contains Rb, which can be explained by its later crystallization with respect to KFsp.

CHEMICAL COMPOSITION OF TRACHYDACITES AND TRACHYRHYOLITES

Petrochemically (Table 3), the rocks are classed with acid (SiO_2 62–76 wt %), low-Fe (Fe_2O_3 + MgO up to 3.5 wt %), peraluminous (A/CNK = 1.28–1.53) rocks, with extremely high potassic alkalinity (from 7.5 to 10.35 wt %) and the practical absence of Ca. It is seen from Table 3 that the highest contents of mafic components and K and Al saturation are typical of the trachydacites with a relatively low SiO_2 content (67 wt % SiO_2). These rocks show the narrowest chemical variations, whereas the rhyolites widely vary in composition, especially in contents of SiO_2 (from 70.5 to 76.7 wt % SiO_2) and K_2O (from 9.66 to 4.96 wt % K_2O), which is presumably related to late silicification. As was mentioned above (Syritso et al., 2005), an increase in the SiO_2 content is accompanied by a decrease in the K_2O content.

Geochemically (Tables 3, 4), these rocks, like the Orlovka granites, have high concentrations of lithophile elements (up to 2400 ppm Rb, up to 950 ppm Li, up to 85 ppm Cs), and, at the same time, are enriched in incompatible elements, similarly to subalkaline basalts of the group of ore deposits (1200 ppm Ba, 90 ppm Zr, 44 ppm Y, and up to 250 ppm total REE). Note that the most homogenous petrochemical composition at wide geochemical variations is typical of the dacites with the lowest SiO_2 content (up to 67.5 wt %). They demonstrate the highest contents of K, rare and rare-earth elements, at the sharp predominance of LREE over HREE [$(La/Yb)_n$ = 10–15], and a well expressed negative Eu anomaly [$(Eu/Eu^*)_n$ = 0.28].

The trachyrhyodacites are similar to the biotite granites of the Khangilay Massif in terms of elevated content of some rare lithophile elements, including Li, Rb, Sc, Ta, Nb, W, Sn, Th, and U, whose content in the trachyrhyodacites is either identical to or exceed those in the biotite granites. In particular, they show a five-fold increase in Li, Cs, and Rb and a four-fold increase in Ba at similar contents of refractory elements (Nb, Ta, REE, and Zr). The main evidence of their geochemical affinity is the similar REE contents and patterns. Note that, compared to the biotite granites of the Khangilay Massif and trachyrhyodacites, the extreme derivatives of the Khangilay Massif, the amazonite granites, are strongly depleted in REE (up to 27.4 ppm), have a low $(La/Yb)_n$ ratio (2.2), and a clealry pronounced Eu anomaly [$(Eu/Eu^*)_n$ = 0.05].

DATA OBTAINED ON MELT AND CRYSTALLINE INCLUSIONS

Melt inclusions were studied in the most typical representative samples in 0.5-mm thick doubly polished

Table 1. Compositions (wt %) of micas from melt and crystalline inclusions in quartz and from the trachyrhyodacites (sample O-902)

Component	Melt inclusions		Crystalline inclusions		Rock			
	Biotite	Phengite–muscovite	Biotite	Biotite	Biotite	Biotite	Phengite–muscovite	Phengite–muscovite
SiO_2	41.60	53.68	32.89	39.38	35.79	36.36	46.25	44.33
TiO_2	0.26	2.08	0.56	1.66	2.20	2.23	0.00	0.00
Al_2O_3	22.08	18.16	15.87	16.08	17.98	18.52	20.42	22.12
FeO	9.60	14.96	13.61	20.30	21.98	22.36	6.95	10.55
MnO	0.33	0.04	0.33	0.49	0.55	0.50	4.01	1.42
MgO	11.42	1.02	16.87	7.39	8.27	8.30	0.17	0.16
CaO	b.d.l.	b.d.l.	0.52	0.09	0.03	0.03	0.00	0.00
K_2O	8.76	6.85	6.96	7.31	8.27	8.21	11.20	10.84
Na_2O	0.24	0.20	0.14	0.10	0.04	0.06	0.23	0.50
Rb_2O	0.04	0.05	b.d.l.	b.d.l.	b.d.l.	0.05	–	–
Nb_2O_3	b.d.l.	b.d.l.	0.15	b.d.l.	b.d.l.	b.d.l.	–	–
Ta_2O_5	b.d.l.	0.05	b.d.l.	0.11	b.d.l.	b.d.l.	–	–
WO_3	0.12	b.d.l.	0.21	0.12	0.05	0.05	–	–
F	1.06	b.d.l.	1.23	0.28	0.33	0.25	–	–
Cl	b.d.l.	0.09	0.05	0.05	0.05	0.05	–	–
Total	95.51	97.18	89.39	93.36	95.53	96.97	89.23	89.92
Numbers of cations normalized to 22 f.u.								
Si	2.98	3.66	2.65	3.03	2.75	2.75	3.45	3.29
Al^{IV}	1.02	0.34	1.35	0.97	1.25	1.25	0.55	0.71
Total Z	4.00	4.00	4.00	4.00	4.00	4.00	4.00	4.00
Ti	0.01	0.11	0.03	0.10	0.13	0.13	0.00	0.00
Al^{VI}	0.84	1.12	0.16	0.49	0.38	0.40	1.25	1.23
Fe	0.57	0.85	0.92	1.31	1.41	1.41	0.43	0.66
Mn	0.02	0.00	0.02	0.03	0.04	0.03	0.25	0.09
Mg	1.22	0.11	2.02	0.85	0.95	0.93	0.02	0.01
Total Y	2.66	2.19	3.13	2.78	2.91	2.90	1.95	1.98
Ca	0.00	0.00	0.05	0.01	0.00	0.00	0.00	0.00
K	0.80	0.60	0.72	0.72	0.81	0.79	1.07	1.03
Na	0.03	0.03	0.02	0.02	0.01	0.01	0.02	0.05
Total X	0.83	0.63	0.79	0.75	0.82	0.80	1.09	1.08
F	0.24	0.00	0.31	0.07	0.08	0.06	–	–

Note: All iron is recalculated in the form of FeO; b.d.l. means concentrations below the detection limit; dashes mean not analyzed.

plates. Quartz phenocrysts account for up to 40 vol% of all phenocrysts and occur as 0.5–2.5-mm rounded grains that are resorbed by the groundmass in the form of deep embayments (Fig. 2g) and occasionally have cryptopegmatite rims. During cataclasis, the monolithic quartz phenocrysts were broken into individual fragments with the granulation and transformations of their margins into a fine-grained (0.01–0.08 mm) aggregate. The examination of quartz grains showed that melt inclusions account for no more than 10% of the total area. Quartz usually contains very small two-phase fluid inclusions. Turbid, brownish, strongly fissured grains with clastic material are scarcer. Quartz with melt inclusions typically forms large (up to 2.5–3 mm) turbid irregularly shaped grains that have distinct contacts with felsitic groundmass. The melt inclusions occur as single, occasionally, paired segregations, mainly of rounded shape, from 10 to 100 μm, in most cases from 30 to 50 μm in size (on average), and are typically confined to the central parts of quartz

Table 2. Chemical composition (wt %) of feldspars from melt and crystalline inclusions in quartz and from trachyrhyodacite

Component	K feldspar									Albite		
	Sample O-902					Sample O-901				Sample O-902		Sample O-901
	MI		CI		Rock	MI		CI	Rock	MI	Rock	MI
	3*	σ	3	σ	1	12	σ	1	1	1	1	1
SiO_2	65.98	0.93	68.52	2.38	65.47	65.49	1.16	65.31	64.21	70.52	69.25	66.96
TiO_2	b.d.l.		b.d.l.		b.d.l.	0.03	0.02	b.d.l.	0.02	b.d.l.	0.04	b.d.l.
Al_2O_3	18.68	0.25	18.58	1.23	18.82	18.63	0.66	18.67	18.35	20.35	20.39	20.67
FeO	0.04	0.01	0.07	0.10	0.05	0.03	0.04	b.d.l.	0.01	0.04	0.04	0.07
MnO	b.d.l.		0.03	0.03	b.d.l.	0.03	0.01	0.03	b.d.l.	0.03	b.d.l.	b.d.l.
MgO	0.03	0.01	0.09	0.15	0.03	0.16	0.36	0.08	0.01	b.d.l.	0.02	0.01
CaO	b.d.l.		b.d.l.		b.d.l.	b.d.l.		b.d.l.	b.d.l.	0.46	0.56	0.24
Na_2O	0.37	0.12	0.23	0.22	0.38	0.37	0.10	0.37	0.64	11.27	11.51	11.41
K_2O	13.97	2.00	11.73	3.55	15.70	15.32	1.06	15.94	15.55	0.23	0.52	0.19
SrO	0.03	0.02	b.d.l.		b.d.l.	0.03	0.03	0.03	b.d.l.	b.d.l.	b.d.l.	b.d.l.
Rb_2O	b.d.l.		0.03		b.d.l.	b.d.l.		b.d.l.	b.d.l.	–	–	–
Cs_2O	b.d.l.		b.d.l.		0.05	0.03	0.01	b.d.l.	0.03	b.d.l.	0.04	b.d.l.
WO_3	0.11	0.07	0.02	0.02	–	0.09	0.11	–	b.d.l.	–	–	b.d.l.
Ta_2O_5	0.05	0.04	0.08	0.12	–	0.04	0.07	–	b.d.l.	–	–	b.d.l.
P_2O_5	0.03	0.02	b.d.l.		b.d.l.	0.05	0.10	b.d.l.	b.d.l.	0.02	b.d.l.	0.02
BaO	b.d.l.		b.d.l.		0.12	0.12	0.02	0.07		0.06	b.d.l.	
Total	99.29		99.38		100.62	100.42		100.49	98.82	102.98	102.37	99.57

Note: All iron as FeO, (MI) melt inclusion, (CI) crystalline inclusion, * number of measurements. σ mean square deviation. b.d.l. means concentrations below the detection limit, dashes mean not analyzed.

grain. The melt inclusions consist of glass (Fig. 2c) or several phases (Figs. 2a, 2b, 2d, 2e): glass, a crystalline phase of double-refracting minerals and a bubble with a fluid phase occupying 10–15 vol %. It can be seen in transmitted light that the melt inclusions from trachydacites consist mainly of a crystallized aggregate and contains brownish hardly discernible low-refraction glass. As is indicated by microprobe analysis, the crystalline phases of the melt inclusions are KFsp, albite, mica, and unidentified ore minerals (?). Dark micas were identified only in the trachydacites. Melt inclusions in quartz from the trachydacites are almost never accompanied by fluid inclusions, whereas those in the Orlovka granites have trails of fluid inclusions. This presumably indicates that quartz in the trachydacites crystallized in magmatic stage, from relatively dry water-undersaturated melts. The crystalline inclusions (from 10 to 30 μm in size) typically contain KFsp (Fig. 2f, 2g), albite, and flakes of mafic mica.

To determine the composition of the parent trachyrhyodacite melt, the partially or completely recrystallized at room temperature melt inclusions were homogenized. For this purpose, the host grains were welded into a gold ampoule, heated in cold-seal pressure vessels, and quenched (rapid quench hydrothermal apparatus) (Badanina et al., 2004). The heating temperature was determined experimentally; the complete homogenization was attained at a temperature of 730–750°C and a pressure of 2 kbar. The experiments lasted for 24–28 h. After the experiments, the melt inclusions consisted of silicate glass with a small bubble, usually in the outer part of the inclusions.

Composition of Melt and Crystalline Inclusions

The composition of the crystalline phases and glasses from partially and completely crystallized melt inclusions (17 inclusions), homogeneous silicate glasses from melt inclusions after the experiments (19 inclusions), crystalline inclusions (14 inclusions) in quartz, and trachyrhyodacite minerals were determined on a Cameca SX-50 microprobe. The results are shown in Tables 1 and 2. The operation conditions were as follows: the acceleration voltage was 15kV, the beam current was 20 nA, the beam size was 5–30 μm, and the counting time was 10 s. Silicate glasses were analyzed with a maximally defocused beam to preclude the loss of alkaline components. It was found out that the crystallized aggregates of melt inclusions and crystalline inclusions contain mainly KFsp and phengite-musco-

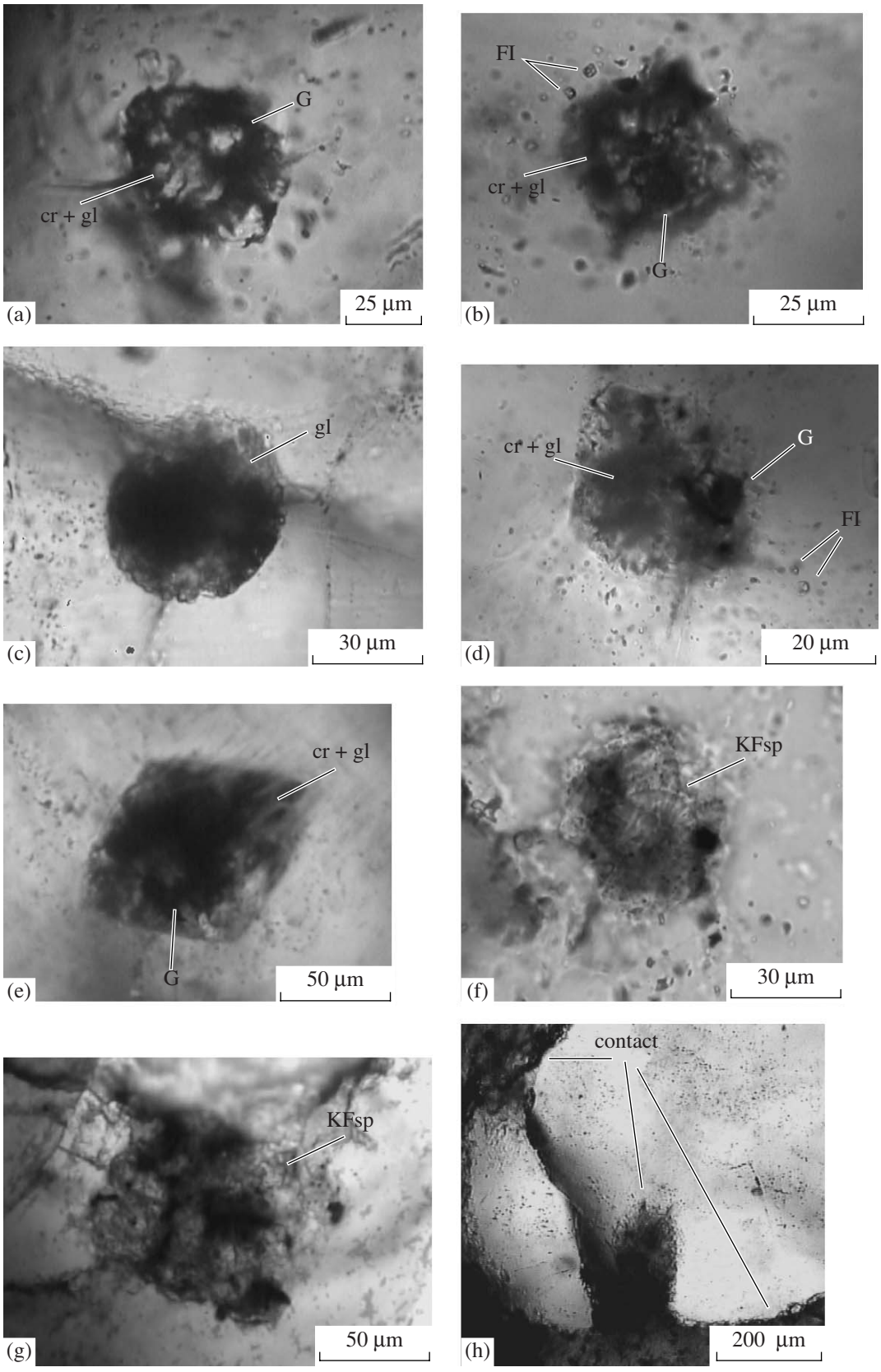

Fig. 2. (a–e) Melt inclusions and (f, g) crystalline inclusions of K feldspar in quartz from trachyrhyodacites and (h) the glassy groundmass forming deep embayment in quartz phenocrysts; (cr) crystalline phase of melt inclusions, (gl) glass, (G) gas bubble, (FI) fluid inclusions.

Table 3. Chemical composition of silicate glasses of melt inclusions and trachyrhyodacites from the Orlovka Massif

Component	Trachydacite			Trachyrhyolite					*Ms-Mc-Ab* granite		Amazonite granite		Topaz rhyolite of Spor Mountain****		Rhyolites of the Tulukuev deposit*****	
	Sample O-902			Sample O-901					Sample O-230		Sample O-626					
	Melt (750°C)		Rock	Glass		Melt (720°C)		Rock	Melt (700°C)		Melt (750°C)		Glass	Melt (700°C)	Glass	Melt
	After homogenization			Prior to		After			After		After		Prior to	After	Prior to	After
				Homogenization					Homogenization							
	6*	σ		6	σ	8	σ		7	σ	6	σ			7	8
SiO_2	66.90	1.13	67.18	60.25	1.18	76.17	1.35	74.10	69.4	1.23	67.00	0.78	65.55	70.10	64.53	72.9
TiO_2	0.09	0.02	0.29	0.11	0.02	0.08	0.04	0.21	0.09	0.02	0.03	0.01	0.02	b.d.l.	0.09	0.11
Al_2O_3	14.04	0.36	16.86	22.87	1.28	12.57	0.69	14.29	15.39	1.08	12.23	0.73	15.42	12.60	18.09	12.16
FeO	2.33	0.43	1.76	0.34	0.14	0.35	0.09	0.70	0.73	0.11	0.67	0.15	0.72	0.50	0.26	0.94
MnO	0.13	0.01	0.23	0.02	0.00	0.08	0.04	0.03	0.25	0.07	0.54	0.18	0.06	0.15	0.11	0.07
MgO	2.68	0.52	1.25	0.04	0.02	0.18	0.05	0.82	0.03	0.02	0.05	0.05	–	–	0.04	0.05
CaO	0.11	0.01	0.05	0.28	0.11	0.07	0.03	0.02	0.53	0.05	0.42	0.46	0.01	0.16	0.06	0.15
K_2O	6.12	0.24	10.28	4.07	0.13	4.51	0.27	7.62	4.00	0.25	2.02	0.34	4.66	4.21	3.78	4.96
Na_2O	1.08	0.00	0.27	6.11	0.09	1.18	0.08	1.01	3.08	0.29	3.70	0.17	6.48	2.91	7.42	4.66
P_2O_5	0.10	0.08	0.06	0.14	0.06	0.03	0.02	0.05	0.03	0.02	0.01	0.01	–	–	b.d.l.	b.d.l.
B_2O_3	b.d.l.		b.d.l.	b.d.l.		b.d.l.		b.d.l.	0.35	0.05	0.89	0.11	–	–	–	–
F	0.04	0.03	b.d.l.	b.d.l.		b.d.l.		0.18	1.33	0.04	1.65	0.07	0.39	1.22	2.99	2.68
Cl	b.d.l.		b.d.l.	0.34		b.d.l.		b.d.l.	0.17		0.01		0.29	0.21	b.d.l.	0.18
L.O.I.			0.80					0.90								
H_2O**	–			–		3.9	0.3		–		8.40	0.50				
Total	93.61		99.03	94.56		99.12		99.93	95.27		97.62		93.62	92.21	97.37	98.86
H_2O***	6.39			5.44					4.73				6.38	7.79	2.63	1.14
A/CNK	1.63		1.45	1.53		1.81		1.44	1.49		1.35		0.98	1.31	1.10	0.91
Rb	274	183	2401	274	183	732	274	618	2650	283	2013	211	–	–	–	–
Sr	85	0	48	254	169	b.d.l.		75	b.d.l.		169	85	–	–	–	19
Nb	159	79	24	477	238	b.d.l.		18	159	79	b.d.l.		–	–	–	–

Note: All iron as FeO. A/CNK = Al/(K + Na + 2Ca).
* Number of measurements, σ means square deviation. ** The H_2O content was determined by Raman spectroscopy. *** Calculated as 100 minus the analytical total; b.d.l means concentrations below the detection limit; dashes mean not analyzed. **** After Tsareva et al., 1991. ***** Chabiron et al., 2001. Oxides, F, Cl, and H_2O are given in wt %; Rb, Sr, and Nb, in ppm.

Table 4. Content of rare and rare earth elements (ppm) in the quench glasses (SIMS) and Orlovka trachyrhyodacites and granites (ICP-MS)

Component	O-902	O-901-2a	O-901	O-133	O-230-4c	O-230-4d	O-230	O-626-4a	O-626
	Trachydacite	Trachyrhyolite		*Bt*-granite	*Ms-Mc-Ab* granite			Amazonite granite	
	rock	Melt	rock	rock	Melt		rock	Melt	rock
Li	951.40	354	181.72	202.80	2397	2411	263.08	544	2288.79
Be	34.02	3.04	4.57	11.64	7.7	13.10	19.25	36	12.89
Ba	1264.28	–	951.79	188.22	–	–	33.55	–	3.65
Nb	23.92	3.64	17.80	34.06	158	26.00	37.05	23.9	268.69
Zr	88.82	–	63.79	57.79	–	–	45.74	–	33.26
Y	32.43	–	39.54	22.76	–	–	49.41	–	3.30
La	45.03	10.74	33.41	36.48	1.25	1.01	11.23	0.18	3.62
Ce	81.87	21.47	58.77	58.35	2.62	1.95	23.90	0.99	13.24
Pr	13.07	2.61	9.56	8.81	0.34	0.3	4.37	0.12	2.16
Nd	46.00	10.98	31.61	29.07	1.24	0.99	15.83	0.34	4.96
Sm	11.40	2.76	7.94	6.61	0.92	0.65	6.48	0.25	2.03
Eu	0.91	6.58	0.77	0.42	0.05	0.03	0.05	0.003	0.00
Gd	8.41	3.53	7.03	5.83	0.96	0.61	6.62	0.18	1.25
Tb	1.37	0.67	1.14	0.93	0.34	0.22	1.41	0.06	0.29
Dy	7.69	3.42	7.5	4.40	1.86	1.44	9.44	0.37	1.36
Ho	1.48	0.72	1.6	0.86	0.34	0.24	1.86	0.05	0.19
Er	4.21	1.41	4.77	2.22	0.81	0.65	4.94	0.16	0.64
Tm	0.64	0.22	0.68	0.32	0.15	0.11	0.85	0.04	0.11
Yb	4.30	1.57	4.51	2.63	1.06	0.76	6.00	0.24	0.78
Lu	0.64	0.22	0.68	0.33	0.15	0.11	0.84	0.04	0.15
Σ REE	227.02	66.89	169.97	157.26	12.1	9.07	93.82	3.00	30.58
$(La/Yb)_n$	6.42	4.19	4.54	9.78	0.82	1.45	1.18	0.52	2.13
Eu/Eu*	0.28	6.61	0.32	0.21	0.16	0.26	0.02	0.04	0

Note: dashes mean not analyzed.

vite, less common albite, while biotite was identified only in the trachydacites.

In the trachydacites, KFsp in melt inclusions, crystalline inclusions, and rocks has the same composition (Table 2) with an insignificant sodic admixture, varying from 0.23 to 0.81 wt % Na_2O. The highest Na_2O contents were found in KFsp from trachyrhyolites. The contents of Rb, Sr, and Ba in KFsp are at the detection limit and were reliably measured only in KFsp from melt inclusions in trachydacites (up to 0.04 wt % Rb_2O). KFsp from the melt inclusions is noted for elevated contents of W and Ta: up to 0.19 wt % WO_3 and 0.09 wt % Ta_2O_5 in the trachydacites and up to 0.34 wt % WO_3 and 0.18 wt % Ta_2O_5 in the trachyrhyolites. KFsp of the crystalline inclusions in quartz from the trachydacites has a lower W content (up to 0.03 wt % WO_3) and a higher Ta content (up to 0.21 wt % Ta_2O_5). KFsp from melt inclusions in quartz from the trachyrhyolites has elevated P_2O_5 contents (up to 0.33 wt %).

Both varieties of the trachyrhyodacites contain subordinate amounts of albite in melt inclusions and rock but not as crystalline inclusions. The mineral contains insignificant admixtures of Ca (from 0.24 to 0.56 wt % CaO) and K (from 0.19 to 0.52 wt % K_2O) (Table 2).

Biotite was found in the melt and crystalline inclusions in quartz and in the rock only in the trachydacites. As is seen in Table 1, biotite has a stable composition in the rock but shows significant variations in the Mg, Fe, and Al concentrations in the inclusions. The highest-Mg biotite was found in the crystalline inclusions. It is also distinguished for the highest contents of trace elements: W (up to 0.21 wt % WO_3), Ta (up to 0.11 wt % Ta_2O_5), Nb (up to 0.17 wt % Nb_2O_5), and Rb (up to 0.05 wt % Rb_2O); the contents of these elements in biotites from the groundmass are at the detection limit. The F content in the biotite from melt inclusions reaches 1.23 wt %, whereas biotite from the rock contains only 0.31 ± 0.02 wt % F at up to 0.09 wt % Cl. It

should be emphasized that the highest F contents were found in the highest-Mg biotite (MgO = 16.87 wt %). The highest Fe content was found in biotite from the rock (FeO_{tot} = 22.36 wt %, TiO_2 = 2.23 wt %).

Composition of Melt Inclusions from the Trachyrhyodacites prior to and after Their Homogenization

Table 3 lists chemical analyses (including F and Cl) of glasses from melt inclusions prior to and after the homogenization of the glasses of melt inclusions from the trachydacites and trachyrhyolites. Since homogeneous and residual glasses of melt inclusions have extremely low contents of mafic components and calcium, the compositional variations of glasses can be explained within the scope of the *Qtz–Ab–Or* system (Fig. 3). Three compositional types of glasses were found (Table 3).

The residual glass in the partially crystallized inclusions from trachyrhyolites prior to their homogenization has the most unusual composition. The residual glass presumably represents the pseudobinary albite–orthoclase system, which preserved, owing to its rapid quench, equilibrium between the Na-rich melt and noninteracting KFsp. This glass contains only 60.25 wt % SiO_2 at high Al_2O_3 (22.87 wt %) and high Na_2O (6.11 wt % K_2O) contents, which significantly predominates over K_2O (4.07 wt %). This glass is characterized by extremely low contents of mafic components and basicity but has a relatively high Cl content (up to 0.34 wt %) and contains no F.

The composition of homogenized glasses from the trachyrhyolites and the trachydacites are petrochemically similar to the bulk rock composition: they are highly silicic (66.90–76.17 wt % SiO_2) and have a low mafic index, with K dominating over Na (3.51–6.12 wt % K_2O and 1.08–1.18 wt % Na_2O). Melts from both of these rocks, like the rocks themselves, differ in composition: compared to the trachydacites the trachyrhyolites, as have a higher SiO_2 content, lower Fe and Mg contents, and higher total alkalis at the strong predominance of K (6.12 ± 0.24 wt % K_2O).

In the *Qtz–Ab–Or* diagram (Fig. 3), the compositions of the melts prior to their homogenization occupy the extremal position, maximally approaching the *Ab* corner, as compared to known natural and experimental systems. The homogenized melts have a principally different composition, forming a compact field along the *Qtz–Or* side. The compositions of melts from the trachydacites are close to the *Or* corner, while melts from the trachyrhyolites are shifted toward the *Qtz* corner.

The comparison of the Orlovka trachyrhyodacite with the known rhyolites of the Streltsovka caldera (Chabiron et al., 2001), which are spatially related to the largest uranium deposit of eastern Transbaikalia, shows a significant difference between the compositions of their parent melts at a high degree of their fractionation in both cases. Judging from the data in Table 3, the melt of the Orlovka trachyrhyodacites is super-peraluminous (A/CNK = 1.53–1.81), whereas the melt of the Streltsovka rhyolites is moderately agpaitic (A/CNK = 0.88–1.10). The latter is characterized by higher total alkalinity ($Na_2O + K_2O \sim 10$ wt %) as compared to the former melt ($Na_2O + K_2O < 8$ wt %). The melt of the Streltsovka rhyolites was relatively dry (no more than 2.4 wt % H_2O, direct determination) and had a high F content (from 1.4 to 2.7 wt %), whereas the melt of the Orlovka trachyrhyodacites had a low F content, around the detection limit (0.04 wt %), and was water-rich, judging from the low analytical totals (with a deficit of 6.4 wt%). The comparable melts differ in geochemistry. The melts of the Orlovka trachyrhyodacites contain up to 1000 ppm Rb, 354 ppm Li. In contrast, the melt of the Streltsovka rhyolites is enriched in refractory elements incompatible with felsic melts: Nb (up to 202.7 ppm) and REE (ΣREE = 299 ppm) as compared to 66.89 ppm and 3.64 ppm, respectively, in the Orlovka trachyrhyolites. Thus, the melt of the Orlovka rhyolites geochemically corresponds to peraluminous rare-metal granites, whereas the melt of the Streltsovka rhyolites is close to rare-metal agpaitic granites.

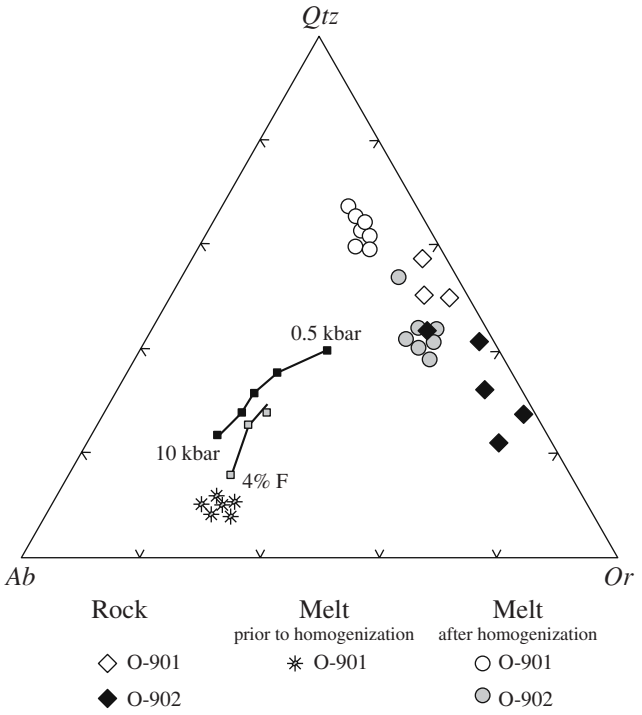

Fig. 3. Compositions of rocks and melts in the *Ab–Qtz–Or* diagram.

Composition of Bulk Rocks and Melt Inclusions

The composition of melt inclusions prior to their homogenization principally differs from the bulk rock composition in having a lower SiO_2 content, extremely high saturation with Al (A/CNK = 1.53), Na predomi-

nance over K (Na/K= 0.14), at high total alkalinity. The homogenized melts are principally similar to the bulk composition of the corresponding rocks: trachydacites and trachyrhyolites. The homogenized melt inclusions have a higher SiO_2 content (66.90 wt % SiO_2 in melt inclusions from the trachydacites and 76.17 wt % SiO_2 in melt inclusions from the trachyrhyolites) as compared to the corresponding rocks (67.18 wt % SiO_2 in the trachydacites and 74.10 wt % SiO_2 in the trachyrhyolites), which can obviously be explained by some overheating of the inclusions and the dissolution of the host quartz, although, the homogenized glass was analyzed in the central part of large inclusions to avoid the trapping of melted material. As is seen in Table 3 and Fig. 3, the homogenized melts of the trachydacites and trachyrhyolites have a significantly lower K content as compared to the bulk composition of the rocks. In particular, the K content in the trachydacite melt corresponds to 6.12 wt % K_2O, while the rock usually contains >10 wt % K_2O. The melts are higher in Na and significantly lower in Al (by 2% Al_2O_3). The trachydacite melt is more mafic than the rock, whereas trachyrhyolite melt has lower Mn and Fe concentrations than the rock. However, the main difference is that the melt shows low analytical totals, which are deficient for about 6.4 wt % in the trachydacites, presumably due to a water content in the melt. Raman spectroscopy determination of the water content in the trachyrhyolite melt shows 4.2 wt % H_2O. In this case, the totals of the analyses are close to 100 wt %, which serves as indirect evidence of the absence of other volatiles in the melt.

A significant fact is that the rock and melt strongly differ in Rb and Li contents. As is seen in Table 3, the trachydacites are almost one order of magnitude richer in Rb than the melt (274 and 2401 ppm, respectively). The melt of the trachyrhyolites is higher in Rb (732 ppm), whereas the rocks do not accumulate it. The ion-microprobe Li content (Table 4) accounts for 354 ppm in the trachyrhyolites, which is almost two times more than its content in the rock (182 ppm). The different distribution of Rb and Li, elements that behave similarly, suggests that host quartz crystallized from the melt inclusions after KFSp, which is the main Rb carrier.

REE Content in the Melt, Trachyrhyodacite, and Rare Metal Granites of the Orlovka Massif

As was mentioned above (Syritso et al., 2005), the trachyrhyodacites and biotite granites of the Khangilay intrusion have similar LREE contents and distribution. As compared to the biotite granites, the trachyrhyodacites have higher HREE, while their distribution pattern is similar to that of the porphyroblastic microcline–albite granites, the late phase of the rare-metal granites. The rocks of the vertical differentiates of the Orlovka Massif form a series of REE patterns, which indicates a subsequent decrease in the total REE (from 157.26 to 30.58 ppm) and increase in the Eu anomaly [$(Eu/Eu^*)_n$ from 0.21 to 0] at a similar shape of the REE patterns, which are inherited from the porphyroblastic granites. Such a significant range in the REE contents confirms the intense fractionation of the parent melt of the Orlovka massif. The melts of both trachyrhyodacites and granites have low REE contents, which is presumably related to early REE accumulation in accessory minerals. This difference becomes especially significant for granite melts (Badanina et al., 2006), whose derivatives contain only 3 ppm REE. At the same time, as is shown in Fig. 4, the melt of amazonite granites shows a higher deficit in Eu^{2+} with distinct first and third tetrads (T_1, T_3). This fact indicates that the tetrad effect occurred in the silicate volatile-rich melt regardless of the hydrothermal–metasomatic processes, as was suggested previously. As can be seen in Fig. 4, the REE distribution pattern of the trachyrhyolite melt is similar to that of the rock at somewhat lower REE contents and a positive Eu anomaly [$(Eu/Eu^*)_n = 6.61$] in the melt.

DISCUSSION AND CONCLUSIONS

Our study confirmed the existence of a high-K peraluminous silicate melt. Two independent types of melts were identified: a felsic melt (76.2 wt % SiO_2) responsible for the formation of trachyrhyolites and an intermediate melt (66.9 wt % SiO_2) that produced trachydacites. The petrochemical compositions of the homogenized glasses appeared similar to those of the corresponding rocks. It is worth noting that the highest K content (K_2O = 6.12 wt %, on average, at Na_2O = 1.08 wt %) is typical of the low-Si melt, whereas the felsic melts (76.17 wt % SiO_2) contain no more than 4.51 wt % K_2O. This difference becomes more contrasting while comparing the bulk rock composition. In particular, the trachydacites contain up to 10 wt % K_2O at the practical absence of Na_2O, whereas trachyrhyolites contain no more than 7,25 wt % K_2O. The main difference of these melts from the bulk rocks is the elevated water content (up to 4.2 wt % H_2O) in the trachyrhyolite melt.

The melts were initially enriched in rare lithophile elements. In particular, the microprobe Rb content is as high as 1000 ppm, while the Li content determined by ion microprobe accounts for 354 ppm. The difference in the contents of rare elements and potassium between the melt and rock is possibly related to the effect of the Orlovka Massif on the studied rocks. However, the time and character of this effect is controversial, because no signs of intense metasomatic alteration were detected in the contact aureole of the Orlovka Massif. Nevertheless, the Li distribution during evolution of the melt of the Orlovka Massif is quite remarkable. As is shown in Table 4, the highest Li contents (2397 ppm) were found in the melt of deep-seated muscovite microcline–albite granites, whereas the melts of amazonite granites from the outercontact zone contain no more than 544 ppm Li. The rocks show the opposite relations: strong Li accu-

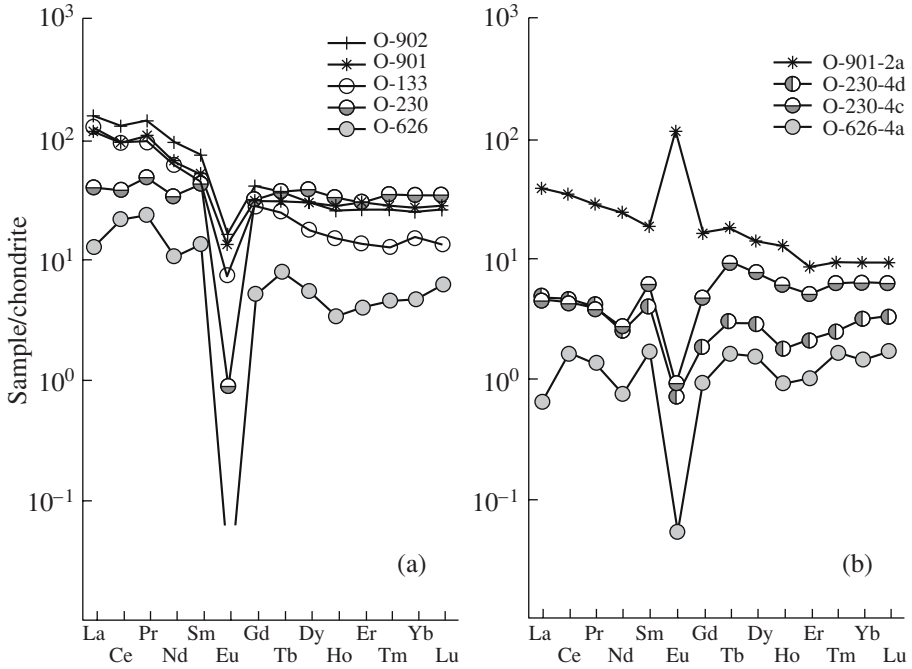

Fig. 4. Chondrite-normalized (Sun and McDonough, 1989) REE patterns.
(a) Trachyrhyodacite (O-902), trachyrhyolite (O-901), biotite granite (O-133), porphyroblastic muscovite–microcline–albite granite (O-230), and lepidollite–amazonite–albite granite (O-626) of the Orlovka Massif (b), in the melt of trachyrhyolite (O-901-2a), muscovite–microcline–albite (O-230-4c and O-230-4d) and lepidolite–amazonite–albite granite (O-626-4a) of the Orlovka Massif.

mulation in the amazonite granites (2288 ppm) at only 263.08 ppm Li in the least differentiated deep-seated granites. Such an inversion in the Li distribution in the rock and melt may indicate that a Li-rich melt or fluid was exsolved and transported to upper levels, and this caused secondary Li accumulation in the apical part of the Orlovka Massif. Conceivably, some of these fluids could also enrich the near-contact trachyrhyodacites containing 951.4 ppm Li.

The melts of the Orlovka trachydacites are noted for low F content (0.07 wt %), whereas the trachyrhyolite melt does not contain F at the detection limit of 0.05 wt %. As is seen in Table 3, the rocks show an opposite pattern: the trachydacites are devoid of F, whereas the trachyrhyolites contain 1800 ppm F. This trend was highlighted during the study of the F distribution in mica in a series of melt inclusions–crystalline inclusions–rock. As is seen in Table 1, the highest F contents were discovered in the highest Mg early biotite from melt inclusions in quartz from the trachydacites, while the F content decreases with increasing Fe mole fraction of micas (from 1.23 wt % in biotite from melt inclusions to 0.22 wt % in biotite from the rock). The trachyrhyolites contain no biotite, but bear their own F carriers: topaz and F-bearing phengite–muscovite.

The residual melt has the most unusual composition. It is characterized by an extremely low mafic index and basicity (< 0.5 wt % mafic oxides), high saturation with Al (A/CNK = 1.53), comparatively low SiO_2 content (SiO_2 = 60 wt %), high total alkalinity (> 10 wt % $K_2O + Na_2O$) at significant Na_2O predominance over K_2O (6.11 wt % Na_2O). In the *Qtz–Ab–Or* diagram, the compositions of these melts occupy an extreme position, being the closest to the *Ab* corner compared to the known natural and experimental systems. In contrast, the compositions of the homogenized melts occupy a principally different position, forming compact fields along the *Qtz–Or* side. The compositions of trachydacites are close to the *Or* corner, while trachyrhyolites are shifted toward the *Qtz* corner. The comparison of the compositions of residual glasses (prior to homogenization) with those of homogenized quench glasses from the rhyolites of the Orlovka Massif (this study), Streltsovka caldera (Chabiron et al., 2001), Spor Mountain, US (Tsareva et al., 1991) highlights similar trends, which are expressed in a higher SiO_2 content and, respectively, a lower Al_2O_3 content in the quench glasses. Note that this trend is accompanied by an inversion in the alkali ratio: the residual glasses have mainly sodic composition, whereas quench glasses are dominated by K. The composition of the residual melt of the Orlovka trachyrhyolites well corresponds to ongonite magma, with the exception of the absence of F and, in contrast, the presence of a high Cl content (up to 0.34 wt %). The presence of such a rare-metal enriched residual melt indicates that the magma differentiation of the Orlovka trachyrhyodacites followed the ongonite trend with the accumulation of volatiles, primarily, water, chlorine, and rare metals in the residual melts. In this case, the primary melt presumably corre-

sponded to a more mafic dacite composition, whereas the rhyolite melt was presumably produced by the partial melting of a shale–schist sequence by dacite melt, which led to an increase in SiO_2 content, decrease in K_2O, rare alkali metals, REE, and F.

Our data demonstrated the potential possibility of the appearance of an unusual residual Cl-bearing ongonite-like melt during the fractional crystallization of the trachyrhyodacite magma. However, these questionable melts cannot be related to the rare-metal granites of the Orlovka Massif, because their formation was separated by a significant time gap of 90 Ma. The age relations between the granites of the Khangilay intrusion and trachyrhyodacite were estimated by U–Pb local dating on zircons. The studies were conducted on a high-resolution SHRIMP-II secondary ion microprobe with mass-spectrometric termination at the Center of Isotopic Research of the Karpinskii All-Russia Research Institute of Geology. The results of these investigations will be reported in another paper. Note only that the obtained data showed that the biotite granites of the Khangilay and Orlovka massifs were formed practically simultaneously at 140.3 ± 2.6 Ma and 140.6 ± 2.9 Ma, respectively. Their simultaneous formation is also confirmed by Rb–Sr dating (139.9 ± 1.9 Ma; Negrei et al., 1995; Kovalenko et al., 1999; Kostitsyn et al., 2004), whereas trachyrhyodacites were dated at 235.4 ± 2.4 Ma. Nonetheless, the ubiquitous spatial association of the Li–F granites with rhyolites, the similarity of their geochemical composition, including REE contents and distribution patterns, and the initial Sr isotopic composition suggest that the rare metal granites and trachyrhyodacites were derived from similar protoliths. The rocks of the Khangilay complex could be generated from the sand–shale sequences of the Upper Riphean Onon Formation. This assumption could be made on the basis of the fact that detrital grains and some nuclei of the zircon from the rare-metal granites of the Orlovka Massif and trachyrhyodacites define an age of 789 ± 13 and 530 ± 10 Ma, respectively.

ACKNOWLEDGMENTS

We are grateful to O. Appelt, D. Rhede, and M. L. Wiedenbeck (GeoForschungsZentrum Potsdam) for help in the performance of analytical studies. We thank E. V. Tolmacheva (Karpinskii All-Russia Research Institute of Geology) and E. V. Volkova (Scientific Research Institute of the Earth Crust) for consultations and fruitful discussions. The study was supported by the Russian Foundation for Basic Research (project nos. 03-05-65293, 05-05-64878, 05-05-79114), grant BRHE-CRDF (Y2-G-15-03) and GFZ (Potsdam Germany).

REFERENCES

1. V. S. Antipin, K. Kholls, M. A. Mitichkin, et al., "Elvans of Cornwall (England) and South Siberia: Subvolcanic Analogues of the Subalkaline Rare-Metal Granites," Geol. Geofiz. **43** (9), 847–857 (2002).
2. E. V. Badanina, R. B. Trumbull, P. Dulski, et al., "The Behavior of Rare-Earth and Lithophile Trace Elements in Rare-Metal Granites: A Study of Fluorite, Melt Inclusions and Host Rocks from the Khangilay Complex, Transbaikalia, Russia, "Can. Mineral. **44**, 667–692 (2006).
3. E. V. Badanina, I. V. Veksler, R. Thomas, et al., "Magmatic Evolution of Li–F Rare-Metal Granites: A Case Study of Melt Inclusions in the Khangilay Complex, Eastern Transbaikalia (Russia), " Chem. Geol. **210**, 113 (2004).
4. S. M. Beskin, A. M. Grebennikov, and V. V. Matias, "Khangilay Granite Pluton and the Related Orlovka Tantalum Deposit, Transbaikalia, Russia," Petrologiya **2**, 68–87 (1994).
5. D. M. Burt, M. F. Sheridan, J. V. Bikun, and E. H. Christiansen, "Topaz Rhyolites—Distribution, Origin and Significance for Exploration," Econ. Geol. **77**, 1818–1836 (1982).
6. A. Chabiron, A. P. Alyshin, M. Cuny, et al., "Geochemistry of the Rhyolitic Magmas from the Streltsovka Caldera (Transbaikalia, Russia): A Melt Inclusion Study," Chem. Geol. **175**, 273–290 (2001).
7. E. H. Christiansen, M. F. Sheridan, and D. M. Burt, "The Geology and Geochemistry of Cenozoic Topaz Rhyolites from the Western United States," Geol. Soc. Amer. Spec. Pap. **205**, (1986).
8. V. B. Dergachev, "Classification of Rare-Metal Ongonite-Group Rocks," Geol. Geofiz., No. 2, 104–112 (1992).
9. V. B. Dergachev, "Cs Variety of the Ultrare Rare-Metal Granite Porphyry (Elvans)," Dokl. Akad. Nauk SSSR **305** (3), 708–712 (1989).
10. W. T. Kortemeir and D.M. Burt, "Ongonite and Topazite Dikes in the Flying Wrench Area, Tonto Basin, Arizona," Am. Mineral. **73**, 507–523 (1988).
11. Yu. A. Kostitsyn, Yu. P. Zaraiskii, A. M. Aksyuk, et al., "Rb–Sr Evidence for the Genetic Links between Biotite and Li–F Granites: An Example of the Spokoinoe, Orlovka, and Etyka Deposits, Eastern Transbaikalia," Geokhimiya, No. 9, 940–948 (2004) [Geochem. Int. **42**, 822–829 (2004)].
12. V. I. Kovalenko and N. I. Kovalenko, *Ongonites as Subvolcanic Analogues of the Rare-Metal Li–F granites* (Nauka, Moscow, 1976) [in Russian].
13. V. I. Kovalenko, Yu. A. Kostitsyn, V. V. Yarmolyuk, et al., "Magma Sources and the Isotopic (Sr and Nd) Evolution of Li–F Rare-Metal Granites," Petrologiya **7**, 401–429 (1999) [Petrology **7**, 383–409 (1999)].
14. V. D. Kozlov, L. I. Reif, and V. V. Skripkina, "Ultrapotassic Differentiation of Subalkaline Rare-Metal Granites (Selengites) and their Exploration Significance," Dokl. Akad. Nauk SSSR **273** (4), 973–976 (1983).
15. A. V. Krivitskii, V. Yu. Izmest'ev, S. V. Misharin, et al., *Report of the Agin Expedition on the Advance Lithochemical Survey on a Scale 1:200 000 in the Onon River Basin for 1999–2001* (FGUP "Chitageols'emka," Chita, 2001) [in Russian].
16. V. B. Naumov, V. I. Kovalenko, R. Klokk'yatti, and I. P. Solovova, "Crystallization Conditions and Phase

Composition of Melt Inclusions in Quartz from Ongorhyolites," Geokhimiya, No. 4, 451–464 (1984).

17. E. V. Negrei, A. Z. Zhuravlev, V. I. Kovalenko, V. V. Yarmolyuk, et al., "Isotopic (Rb–Sr, $\delta^{18}O$) Studies of the Dome of Tantalum-Bearing Li–F Granites," Dokl. Acad. Nauk **342**, 522–525 (1995).
18. M. Pichavant, J. Valencia Herrera, S. Boulmier, et al., "The Macusani Glasses, SE Peru: Evidence of Chemical Fractionation in Peraluminous Magmas," in *Magmatic Processes: Physico-Chemical Principles*, Ed. by B. O. Mysen, Geochem. Soc. Spec. Publ. **1**, 359–373 (1987).
19. S.-S. Sun and W. F. McDonough, "Chemical and Isotope Systematics of Oceanic Basalts: Implications for Mantle Composition and Processes," in *Magmatism in the Ocean Basins,* Ed. by A. D. Saunders and M. J. Norry, Geol. Soc. Spec. Publ. **42**, 313–345 (1989).
20. L. F. Syritso, E. V. Tabuns, E. V. Volkova, et al., "Model for the Genesis of Li-F Granites in the Orlovka Massif, Eastern Transbaikalia," Petrologiya **9**, 313–336 (2001) [Petrology **9**, 268–290 (2001)].
21. L. F. Syritso, E. V. Volkova, E. V. Badanina, and V. S. Abushkevich, "Specific Enriched Ultrapotassic Trachyrhyodacites in the Area of the Orlovka Li–F Granites in Eastern Transbaikalia and the Problem of Their Relation to Rare-Metal Granites," Petrologiya **13**, 133–137 (2005) [Petrology **13**, 95–98 (2001)].
22. A. V. Titov, A. G. Vladimirov, S. A. Vystavnoi, and L. N. Pospelova, "Extraordinary High-Temperature Felsite Porphyries in the Postgranite Dike Swarm of the Kalguty Rare-Metal Granite Massif, Gornyi Altai Mountains," Geokhimiya, No. 6, 677–682 (2001) [Geochem. Int. **39**, 615–620 (2001)].
23. G. M. Tsareva, V. B. Naumov, V. I. Kovalenko, et al., "Composition and Crystallization Conditions of the Topaz Rhyolites of the Spor Mountain, USA: Data on Melt Inclusions," Geokhimiya, No. 10, 1453–1462 (1991).
24. J. D. Webster, D. M. Burt, and R. A. Aguillion, "Volatile and Lithophile Trace-Element Geochemistry of Heterogeneous Mexican Tin Rhyolite Magmas Deduced from Compositions of Melt Inclusions," Geochim. Cosmochim. Acta **60**, 3267–3283 (1996).
25. J. C. Zhu and H. Zhang, "Geochemical Evolution for Subvolcanic Analogue of Rare Metal-Bearing Li–F-Rich Granites," in *Proceedings of Goldschmidt Conference Abstract, 2003*, p. A585.